JOURNAL OF MATERIALS SCIENCE **39** (2004) 1071–1074

Influence of Al_4C_3 particle volume fraction on fracture mechanism in Al-Al_4C_3 composite

M. BESTERCI
Institute of Materials Research, Slovak Academy of Sciences, Watsonova 47, 043 53 Košice, Slovakia

J. IVAN
Institute of Materials and Machine Mechanics, Slovak Academy of Sciences, Račianska 75, 838 12 Bratislava, Slovakia

O. VELGOSOVÁ
Faculty of Metallurgy, Technical University, Letná 9/A, 042 00 Košice, Slovakia

P. HVIZDOŠ
Institute of Materials Research, Slovak Academy of Sciences, Watsonova 47, 043 53 Košice, Slovakia

The method of *in situ* tensile testing in SEM is suitable for investigations of fracture mechanisms because it enables to observe and document deformation processes directly, by which the initiation and development of plastic deformation and fracture can be reliably described.

In our previous works [1–7] following [8–10] we used this method to analyze deformation processes in various types of Cu and Al based composites. The result was a design of several models of damage, which considered physical parameters of matrix and particles, as well as geometry and distribution of secondary phases.

The aim of the present study is to evaluate the influence of volume fraction of Al_4C_3 particles (8 and 12 vol%) on the fracture mechanism.

The experimental materials were prepared by reaction milling. Al powder of powder particle size of <50 μm was dry milled in an attritor for 90 min with the addition of graphite KS 2,5 thus creating 8 and 12 vol% of Al_4C_3, respectively. The specimens were than cold pressed using a load of 600 MPa, the specimens had cylindrical shape. Subsequent heat treatment at 550 °C for 3 h induced chemical reaction $4Al + 3C \rightarrow Al_4C_3$. The cylinders were then hot extruded at 600 °C with 94% reduction of the cross section. Detailed technology preparation is described in [11, 12].

For the purposes of investigation very small flat tensile test pieces (7×3 mm) with 0.15 mm thickness were prepared by electroerosive machining, keeping the loading direction identical to the direction of extrusion. The specimens were ground and polished down to a thickness of approximately 0.1 mm. Finally, the specimens were finely polished on both sides by ion gunning. The test pieces were fitted into special deformation grips in the scanning electron microscope JEM 100 C, which enables direct observation and measurement of the deformation by ASID-4D equipment.

The microstructures of the materials with 8 and 12 vol% Al_4C_3 were fine-grained (the mean matrix grain size was 0.35 μm), heterogeneous, with Al_4C_3 particles distributed in parallel rows in consequence of extrusion. The average distance between the Al_4C_3 particles, found in thin foils, was 1.1 μm. Besides the phase Al_4C_3, the systems contained also Al_2O_3 phase, which was detected chemically [13, 14]. Essentially, it was the remnant of oxide shells of the original matrix powder and/or shells formed during the reaction milling in attritors. The volume fraction of this phase Al_2O_3 was low, 1–2 vol%.

When describing microstructures, one has to consider geometrical and morphological factors. According to the microstructure observations, the particles in our materials can be divided into three distinctive groups: A—small Al_4C_3 particles, identified by TEM, with mean size approximately 30 nm which made up to 70% of the dispersoid volume fraction; B—large Al_4C_3 particles with mean size between 0.4 and 2 μm, found on metallographic micrographs; and C—large Al_2O_3 particles with mean size of 1 μm. Let us assume that these particles are distributed in parallel rows. Mean distance between the rows is l and between the particles h. The particles are spherical or have only a low aspect ratio, so that they can be approximated as spherical. In [15] it was shown, that for two microstructure states: 1 and 2, which differ only in the distances between the rows of particles (l_1 and l_2), the yield strength relation can be described as

$$\frac{l_1}{l_2} = \frac{\Delta R_{\mathrm{p0.2^1}}}{\Delta R_{\mathrm{p0.2^2}}}, \tag{1}$$

where $\Delta R_{\mathrm{p0.2}}$ is the contribution to yield strength from the dispersed particles.

The experimental materials were deformed at 20 °C at a rate of 6.6×10^{-4} s^{-1} in the elastic region.

In the material with lower volume fraction (8 vol%) of Al_4C_3 with increase of the deformation load the initiation of microcracks on the large Al_4C_3 particles (B) was observed to occur by their rupture simultaneously with decohesion of the smaller Al_4C_3 and Al_2O_3 particles (Fig. 1A and C). The crack then propagated from

0022–2461

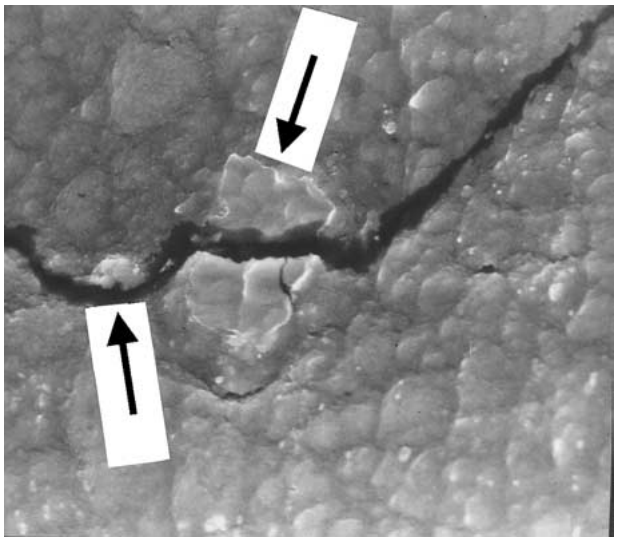

Figure 1 Fracture path in the material with 8 vol% Al_4C_3. Rupture of a large Al_4C_3 grain and decohesion of the smaller particles ($\varepsilon = 0.12$).

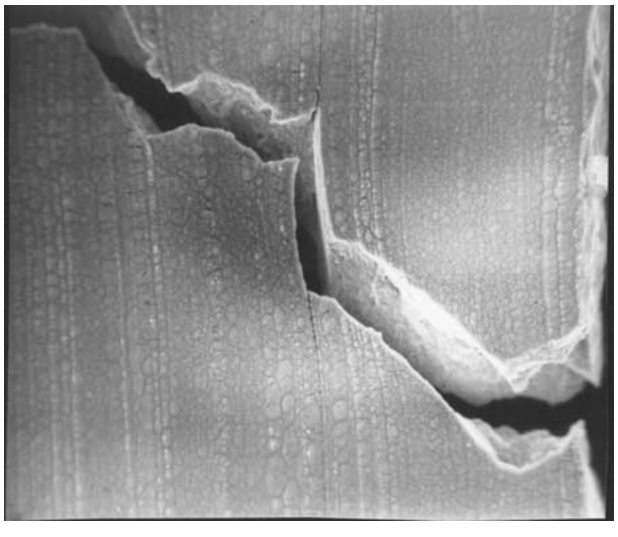

Figure 2 Irregular fracture formed by a crack growing alternatively along the particle rows and between them in the material with 8 vol% Al_4C_3 ($\varepsilon = 0.15$).

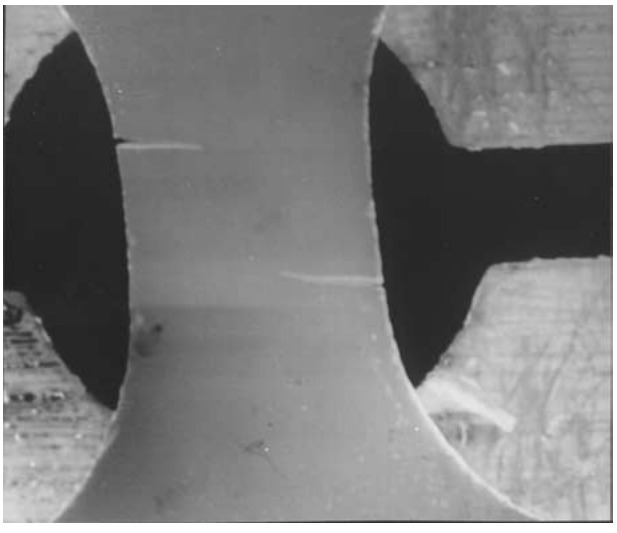

Figure 3 Two cracks initiated on the opposite sides of a specimen. Surface morphology and initiation of cavities in the matrix–particle interphase in the material with 12 vol% Al_4C_3 ($\varepsilon = 0.04$).

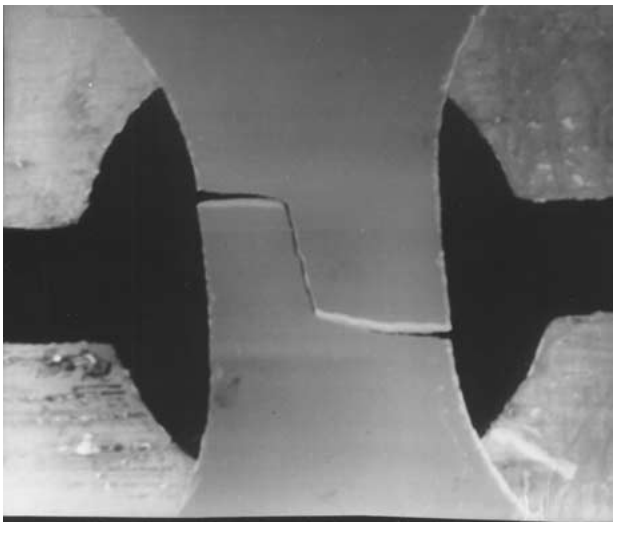

Figure 4 Final fracture by interconnecting the two opposite side cracks in the material with 12 vol% Al_4C_3 ($\varepsilon = 0.05$)

the surface into the bulk of the specimen. On further deformation, as a result of higher concentration of smaller Al_4C_3 particles (A), the perpendicular fracture trajectory partially deviated toward the load direction (Fig. 2) and became irregular.

In the case of the higher volume fraction (12 vol%) of Al_4C_3 the deformation process was very rapid due to the low plasticity of the material. Cracks were initiated on the surface and propagated approximately perpendicularly to the tensile load direction (Fig. 3). Coalescence of the final fracture progressed along densely populated rows of Al_4C_3 (A, B) particles parallel to the load direction (Fig. 4). The fracture surface formed by the crack growth was inclined at 45° with respect to the specimen principal surface. The morphology of the deformed surface and initiation of cavities on the matrix-particle boundaries can be seen in Fig. 5.

A detailed study of the deformation changes showed that the crack initiation was caused by decohesion, and occasionally also by rupture of the large particles. The

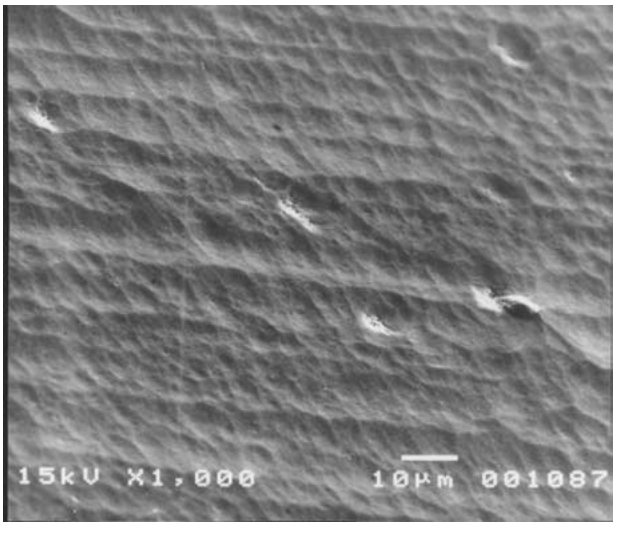

Figure 5 Surface morphology and initiation of cavities in the matrix-particle interphase boundary in the material with 12 vol% Al_4C_3 ($\varepsilon = 0.05$).

decohesion is a result of different physical properties of different phases of the system. The Al matrix has significantly higher thermal expansion coefficient and lower elastic modulus (from 23.5 to 26.5×10^{-6} K^{-1}, and 70 GPa) than both Al_4C_3 (5×10^{-6} K^{-1}, and 445 GPa) and Al_2O_3 (8.3×10^{-6} K^{-1}, and 393 GPa), respectively.

Large differences in the thermal expansion coefficients result in high stress gradients, which arise on the interphase boundaries during the hot extrusion. Since $\alpha_{matrix} > \alpha_{particle}$, high compressive stresses can be expected. However, because the stress gradients arise due to the temperature changes, during cooling (which results in increase of the stress peaks) their partial relaxation can occur. Superposition of the external load and the internal stresses can initiate cracking at interphase boundaries. The fractures of the studied materials started at the side-rims of the deformed samples. When compared to the material with lower volume fraction of Al_4C_3, in the present system the development of slip bands in the bulk was inhibited. This fact, and the absence of long-range slip in the matrix, implies that the fracture is not inclined to the applied load but is perpendicular to it. This is caused by the high volume fraction of the strengthening particles and by their short distance. On the exiguousness of the sample width (0.1 mm), the crack grew at 45 ° with respect to the sample surface. Whether a crack is initiated from a damaged particle or due to boundary decohesion is determined by the particle properties (type, morphology, crystallography, local orientation of the lattice with respect to load), by the manner and kinetics of its creation (*in situ* or admixing to the system), and by the cohesive strength of the matrix-particle boundary. The fracture was transcrystalline, ductile, Fig. 6.

Based on the microstructure changes observed in the process of deformation, the following model of fracture mechanism is proposed (Fig. 7):

(a) The microstructure in the initial state is characterized by Al_4C_3 and Al_2O_3 particles, categorized as A, B, and C, whose geometric parameters (l, h, and d) depend on their volume fraction.

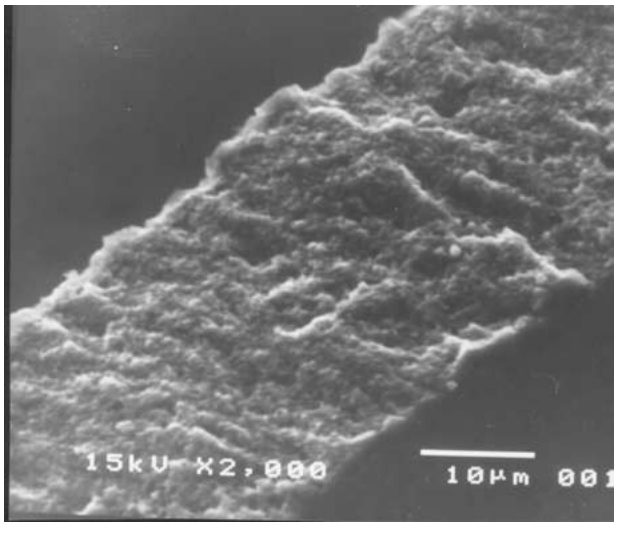

Figure 6 Fine dimples on fracture surface in the material with 12 vol% Al_4C_3.

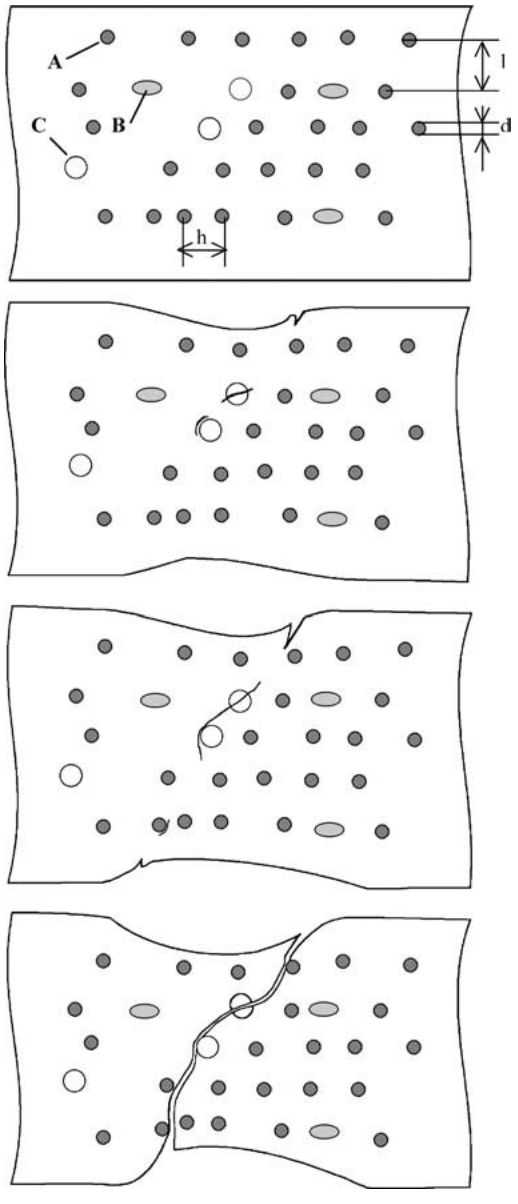

Figure 7 Model of the fracture mechanism.

(b) With increasing tensile load local cracks, predominantly on specimen side surfaces, are formed by rupture of large (B, C) and decohesion of smaller (A) particles.

(c) Further increase of load leads to the crack growth by coalescence of cavities in the direction from the surface to the specimen center. The cracks can be oriented parallel or perpendicular to the loading direction in depending on the particle volume fraction.

(d) The final rupture, i.e., interconnection of the side cracks along the loading direction, takes place in variably dense rows, depending on the volume fractions of carbide (Al_4C_3) and oxide (Al_2O_3) particles.

References

1. M. BESTERCI and J. IVAN, *J. Mater. Sci. Lett.* **15** (1996) 2071.
2. *Idem.*, *ibid.* **17** (1998) 773.
3. M. BESTERCI, J. IVAN, L. KOVÁČ, T. WEISSGAERBER and C. SAUER, *Mater. Lett.* **38** (1999) 270.
4. *Idem.*, *Kovové Mater.* **36** (1998) 239.
5. M. BESTERCI, J. IVAN and L. KOVÁČ, *ibid.* **38** (2000) 21.
6. *Idem.*, *Mater. Lett.* **46** (2000) 181.

7. M. BESTERCI, J. IVAN, O. VELGOSOVÁ and L. PEŠEK, *Kovové Mater* **39** (2001) 367.
8. A. MOCELLIN, F. FOUGEREST and P. F. GOBIN, *J. Mater. Sci.* **28** (1993) 4855.
9. R. VELÍSEK and J. IVAN, *Kovové Mater* **32** (1994) 531.
10. L. V. BROUTMAN and R. H. KROCK, *Compos. Mater.* **5** (1974) 27.
11. G. JANGG, F. KUTNER and G. KORB, *Aluminium* **51** (1975) 641.
12. G. KORB, G. JANGG and F. KUTNER, *Draht* **30** (1979) 318.
13. J. ŠALUNOV, M. ŠLESÁR, M. BESTERCI, H. OPPENHEIM and G. JANGG, *Metall* **6** (1986) 601.
14. H. OPPENHEIM and G. JANGG, and Z. WERKSTOFFTECHNIK **14** (1983) 170.
15. M. BESTERCI and K. PELIKÁN, *Kovové Mater.* **4** (1985) 497.

Received 6 May
and accepted 28 August 2003